JOURNAL OF CATALYSIS **160,** 299–308 (1996)
ARTICLE NO. 0148

Selectivity Enhancement in Methylamine Synthesis via Postsynthesis Modification of Brønsted Acidic Mordenite

An Infrared Spectroscopic and Kinetic Study on the Reaction Mechanism

Christian Gründling, Gabriele Eder-Mirth, and Johannes A. Lercher[1]

Department of Chemical Technology, University of Twente, P.O. Box 217, 7500 AE Enschede, The Netherlands

Received October 19, 1995; revised January 22, 1996; accepted January 24, 1996

Methylamine synthesis from methanol and ammonia over parent and modified Brønsted acidic mordenites is studied by *in situ* infrared spectroscopy and kinetic analysis to elucidate the role of elementary steps for activity and selectivity. *In situ* infrared spectroscopy reveals that all methylammonium ions are formed in the micropores of these catalysts. The formation of the chemisorbed methylamines, however, is not rate determining. Transient response experiments indicate that the desorption of these methylamines aided by adsorbing ammonia and/or the scavenging of methyl groups with ammonia constitutes the rate determining step. For a given catalyst, the selectivity strongly depends on the methanol conversion and the ammonia to methanol ratio of the feed. Upon modification of mordenite with tetraethoxysilane, the selectivity to the lower methylated amines is strongly enhanced. The transport limitations of the bulkier products, formed in high concentration in the pores, are concluded to cause the enhanced selectivity toward mono- and dimethylamine over the modified catalyst. Since a decrease in activity compared to the parent sample was not observed, it seems that the methyl-scavenging mechanism plays an important role over these catalysts.

INTRODUCTION

During the past decades, zeolites have been successfully applied as catalysts for intermediate and fine chemical synthesis (1–3). While the relatively small pores of the zeolites limit their utilization to the synthesis of small molecules, the well-defined and narrow pore size distribution can be used to induce shape selectivity (4–8) by (i) allowing only certain reactants to reach the active sites (*reactant selectivity*) (9), (ii) imposing diffusional constraints on bulkier reaction products (*product selectivity*) (10, 11), or (iii) excluding the formation of certain products due to spatial constraints (*restricted transition state selectivity*) (12).

For the synthesis of methylamines from methanol and ammonia, the thermodynamic equilibrium (as observed over amorphous (silica-)alumina catalysts) favors the formation of trimethylamine (TMA). Since this is the lowest demanded product (13–15), costly recycling procedures of excess TMA become necessary. To enhance the selectivity of acidic catalysts toward monomethylamine (MMA), and dimethylamine (DMA), several molecular sieves were tested. Among them, small pore zeolites (e.g., RHO, ZK-5, and erionite) and mordenites were reported to be the most promising ones (16–23). Substantial improvement was achieved through variation of zeolite morphology and acidity (18, 19). Highly selective formation of MMA and DMA was reported over (partially) cation-exchanged zeolites, but on the expense of drastically lower rates compared with Brønsted acidic molecular sieves.

Recent reports indicate that the selectivity toward the lower substituted methylamines over H–zeolites can be optimized by postsynthesis treatment with sililating agents (i.e., silicon–tetrachloride, tetramethoxysilane, and tetraethoxysilane), while maintaining high activity (24–29). These modifications produce a silica layer at the external surface of the molecular sieve leading to a narrowing of the pore openings (27) and/or (ii) to lower concentrations of acid sites at the external surface (25) than in the parent material.

In this communication, *in situ* infrared (IR) spectroscopy in combination with conventional kinetic analysis is used to address the role of the modification of Brønsted acidic mordenite with tetraethoxysilane for methylamine synthesis. This is achieved by correlating the concentration and type of sorbed species in the mordenite pores of the parent and modified sample with the observed rates and selectivities.

EXPERIMENTAL

Catalyst Preparation

The mordenite (HMOR20) used for this study was supplied by the Japanese Catalysis Society in the ammonium

[1] To whom correspondence should be addressed. Fax: 0031-53-4894683. E-mail: lercher@utct.ct.utwente.nl.

0021-9517/96 $18.00

form (30). Elemental analysis showed the SiO_2/Al_2O_3 ratio to be 20, with extra framework aluminum contributing less than 5% (as determined from ^{27}Al MAS NMR). The average particle size (as determined by scanning electron microscopy) was 1 μm. The number of accessible Brønsted acid sites (1.3×10^{-3} mol/g) was determined gravimetrically by measuring the amount of irreversibly adsorbed ammonia at 373 K (under the assumption of a 1:1 adsorption stoichiometry under these conditions).

For the postsynthesis modification, 1 g of the activated mordenite was suspended in 25 ml *n*-hexane at room temperature. Then, tetraethoxysilane was added, the amount of which was calculated to result in a weight gain of 4% under the assumption that SiO_2 is formed. After 1 h of intense stirring at room temperature, the solvent was removed by evaporation, and the remaining powder (HMOR20-M) was calcined in synthetic air for 2 h at 773 K. Upon this modification, the amount of extra framework aluminum of the mordenite increased to 10%, and the number of accessible Brønsted acid sites was reduced slightly to 1.1×10^{-3} mol/g.

Kinetic Measurements

All kinetic measurements were carried out in a plug flow reactor system with a fixed catalyst bed. The catalyst mass varied between 10 and 150 mg. The gas flows (ammonia, helium) were adjusted by mass flow controllers. Methanol was introduced into the system via a syringe pump. The reactor effluent could be stored in a multiposition valve and subsequently analyzed by gas chromatography using a packed column (3-m stainless-steel column packed with 25% carbowax 400 and 2.5% KOH on acid washed Chromosorb W) for separation as described in Ref. (19). Typically, the reaction was carried out at 633 K after activation of the catalyst in flowing He with an increment of 10 K/min up to 823 K and holding this temperature for 1 h. A partial pressure of 5×10^3 Pa of each reactant (nitrogen to carbon (N/C) ratio = 1) was applied, balanced with He to atmospheric pressure. For some experiments the ammonia partial pressure was raised to 1.5×10^4 Pa, while keeping the MeOH pressure constant. The variation in total conversion, which is calculated based on methanol consumption, was achieved by varying the residence time. The reported selectivities are based on the concentration of methylamines formed. Thus, the total amine selectivity describes the ratio between the concentration of methylamines and that of all reaction products (which includes also dimethyl ether (DME) as byproduct). The selectivity toward each methylamine is given as the molar ratio between this amine and the sum of all methylamines formed.

In Situ Infrared Spectroscopy

For the *in situ* IR spectroscopic studies, the plug flow reactor was replaced with an IR cell, which approximates a continuously stirred tank reactor with a reactor volume of 1.5 cm^3. This experimental setup allows a simultaneous analysis of the sorbed reactants and products inside the zeolite pores and the products in the gas phase (for details see Ref. (31)). In order to obtain quantitative information on the concentration of the surface species, the IR spectra recorded during the reaction were fitted in the spectral range between 1700 and 1350 cm^{-1} via a multicomponent fit with reference spectra. These reference spectra were obtained by sorbing the individual reactants and products in a vacuum system at reaction temperature and a partial pressure of 1 Pa (32). Under these conditions, reactive sorption of the methylamines (with exception of TMA) could be suppressed.

The same vaccum setup was also used to determine the rate of transport of MMA and DMA in HMOR20 and HMOR20/M. The decrease in intensity of the OH-stretching vibration band attributed to the strong Brønsted acid sites with increasing time on stream was monitored after contacting the activated catalyst with the sorbates. These measurements were performed at 308 K and 10^{-1} Pa, in order to avoid disproportionation reactions, which might occur at reaction temperature upon prolonged exposure of the zeolites to the amines. Diffusion coefficients were calculated according to Crank's approximation for diffusion in a plane sheet (33) and an average particle size of 1 μm.

RESULTS

Kinetic Results

The steady-state amine selectivities (recorded after 3 h on stream at 633 K) over the two investigated catalysts as a function of the total methanol conversion are shown in Figs. 1 and 2. The variation in conversion was achieved by varying the weight hourly space velocity (WHSV [g total feed/g catalyst · h]) in the range of 7.5 to 0.4 h^{-1} for both catalysts. The measurements showed that both catalysts had comparable activity and did not deactivate under the chosen experimental conditions. Note that the activity over HMOR20-M was even slightly higher than over the parent mordenite. In general, DME was the only by-product observed. Only at very short time on stream (<5 min) other byproducts (i.e., formaldehyde, hydrocarbons) were formed.

Over HMOR20 (Fig. 1), the total amine selectivity remained rather constant (80%), and only at high methanol conversion a slight increase was observed. The product selectivity toward the primary amine MMA was high (80%) at low conversion, but decreased drastically on expense of TMA as the conversion increased. TMA was the main product at 85% conversion. The selectivity toward DMA increased only slightly from 16 to 25% upon variation of the methanol conversion from 15 to 90%.

A quite different selectivity pattern was observed over HMOR20-M (Fig. 2). DME was formed to a lesser extent

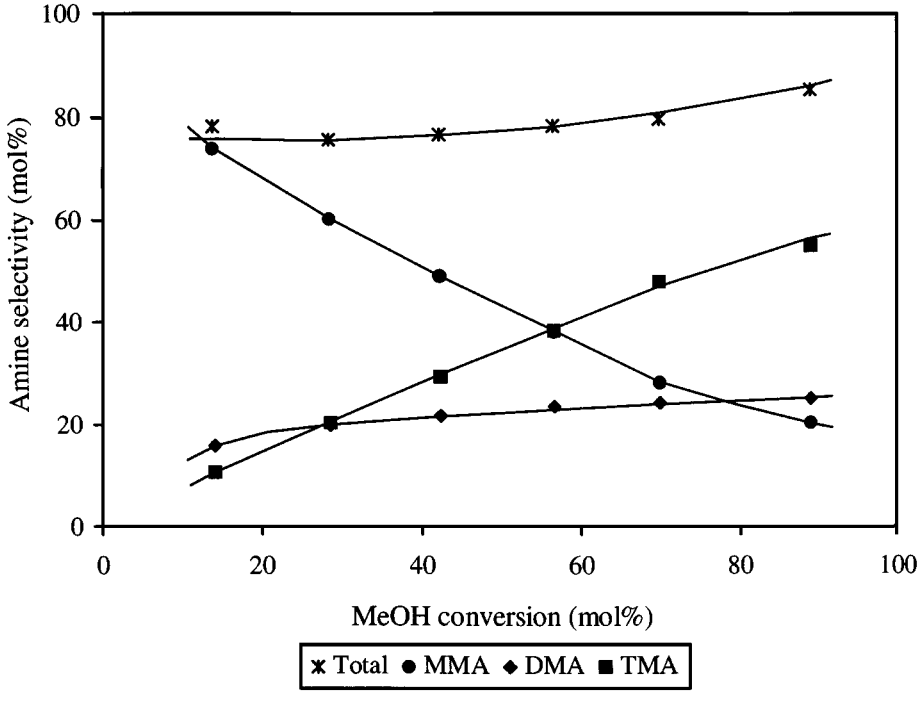

FIG. 1. Amine selectivity over HMOR20 ($P_{(MeOH,NH_3)} = 5 \times 10^3$ Pa, $T = 633$ K) as a function of methanol conversion.

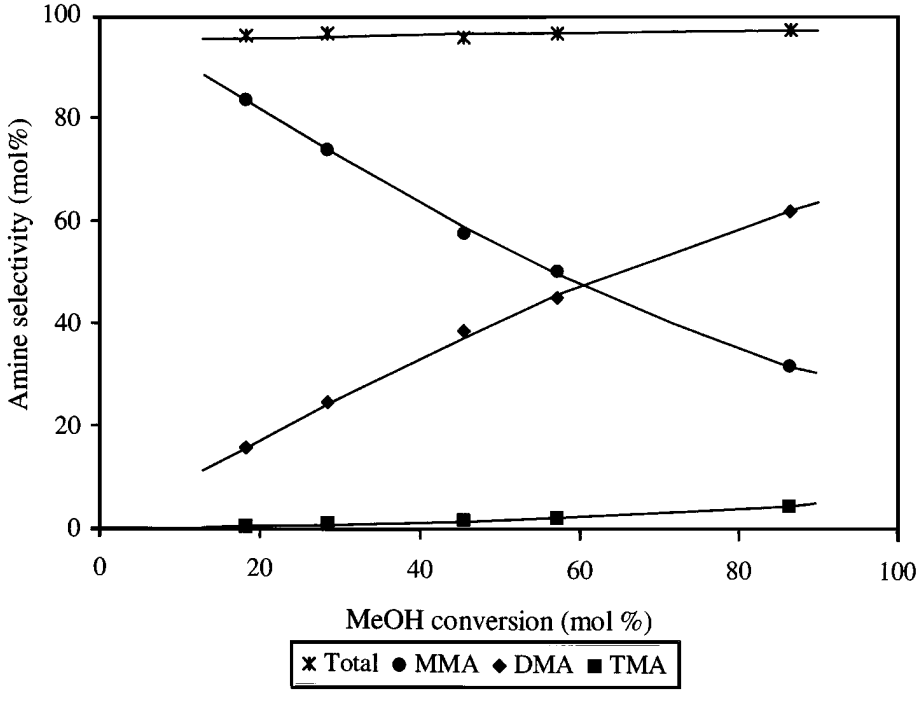

FIG. 2. Amine selectivity over HMOR20-M ($P_{(MeOH,NH_3)} = 5 \times 10^3$ Pa, $T = 633$ K) as a function of methanol conversion.

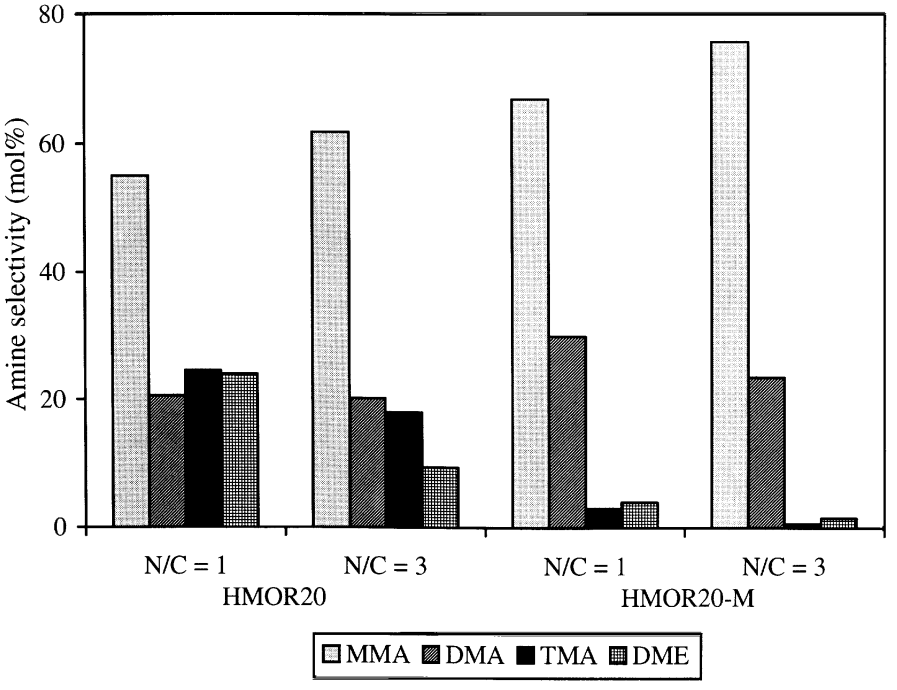

FIG. 3. Amine selectivity over HMOR20 and HMOR20-M ($P_{(NH_3)} = 5 \times 10^3$ Pa, $T = 633$ K), and MeOH conversion = 35%) at different N/C feed ratios.

resulting in a total amine selectivity of more than 95%. Again, at low conversion, MMA was the product with the highest concentration, but its decrease with increasing conversion was paralleled by an increasing in selectivity toward DMA (60% at 85% conversion). At any level of methanol conversion, the formation of TMA was almost completely suppressed (selectivity less than 5%).

At a given conversion, the product distribution can be altered by varying the N/C ratio of the feed. This is shown in Fig. 3, which compiles the product selectivity over both catalysts at 633 K, 35% methanol conversion, and a N/C ratio of 1 and 3. Increasing the concentration of ammonia in the feed slightly enhanced the total catalytic activity (e.g., identical methanol conversions over HMOR20 (35%) was obtained at a WHSV of 2.3 and 2.7 h^{-1} at a N/C ratio of 1 and 3, respectively), while the formation of by-products (i.e., DME) was markedly reduced. Additionally, the selectivity to MMA is enhanced on expense of the higher substituted amines (i.e., DMA, TMA). It should be noted, however, that at a N/C ratio of 3, the concentration of TMA formed over HMOR20 still exceeded that observed over HMOR20-M at a N/C ratio of 1.

In Situ Infrared Spectroscopy

The interaction of methanol and ammonia with HMOR20 under nonreactive and reactive conditions was discussed in detail previously (32). Thus, these results will generally only be cited and included, wherever it is necessary for the discussion.

The IR spectra of HMOR20-M in contact with ammonia and methanol (N/C = 1) at 633 K are depicted in Fig. 4. At very short time on stream, the Brønsted acid sites (3610 cm^{-1}) were completely covered with ammonium ions. With increasing contact time, the band attributed to the NH deformation vibration of ammonium ions (1460 cm^{-1}) quickly decreased in intensity, and new bands, typical for the NH and CH deformation vibrations of chemisorbed, protonated methylamines appeared. All methylamines (up to tetramethylammonium ions (TET)) are formed on the surface as indicated by the presence of IR bands at 1506 cm^{-1} (δ_{NH}(MMA)), 1610 cm^{-1} (δ_{NH}(DMA)), 1470 cm^{-1} (δ_{CH}(TMA)), and 1485 cm^{-1} (δ_{CH}(TET)). It should be emphasized that the Brønsted acid sites remained completely covered, and that sorbed methanol was not detected (detection limit, 5 rel%) under these reaction conditions.

The concentrations of the products and reactants sorbed on HMOR20-M (obtained from a quantitative evaluation of the IR spectra) as a function of time on stream are depicted in Fig. 5. The high initial coverage of ammonia decreased rapidly in favor of sorbed methylamines, which were formed in sequential order. The concentration of chemisorbed MMA and DMA (their highest concentration was already reached after 30 s) passed through a maximum, as these amines constitute also reactants for the next methylation step. A steady-state concentration of surface-bound amines was quickly reached (after 5 min on stream), in which significant amounts of the higher methylated amines (i.e., TMA (20%), TET (31%)) were present.

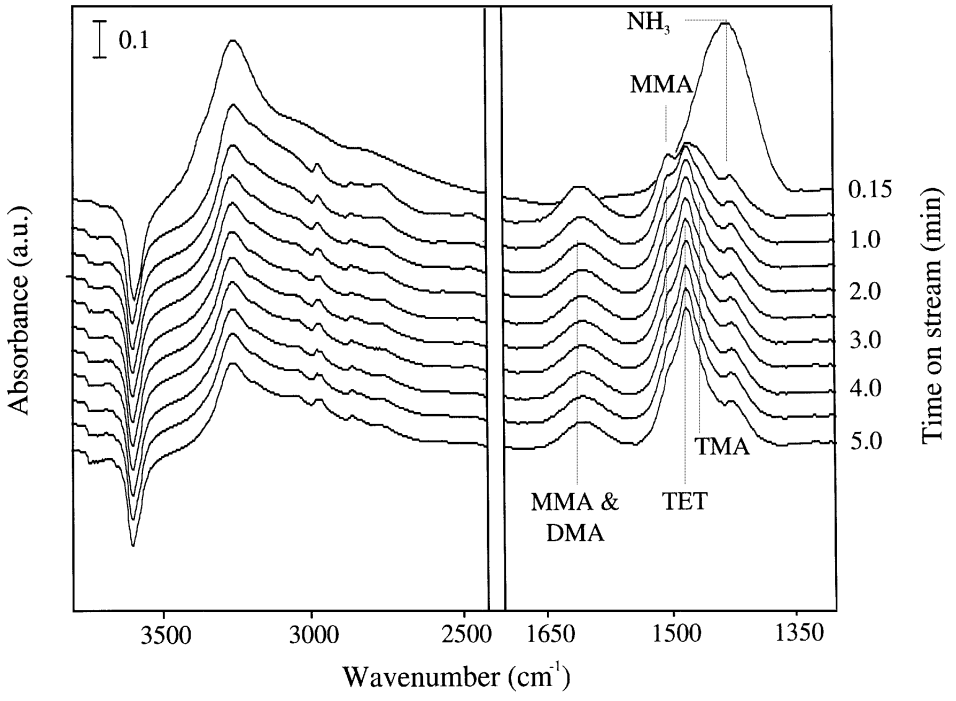

FIG. 4. Time resolved infrared spectra of HMOR20-M under reactive conditions ($P_{(MeOH,NH_3)} = 5 \times 10^3$ Pa, $T = 633$ K).

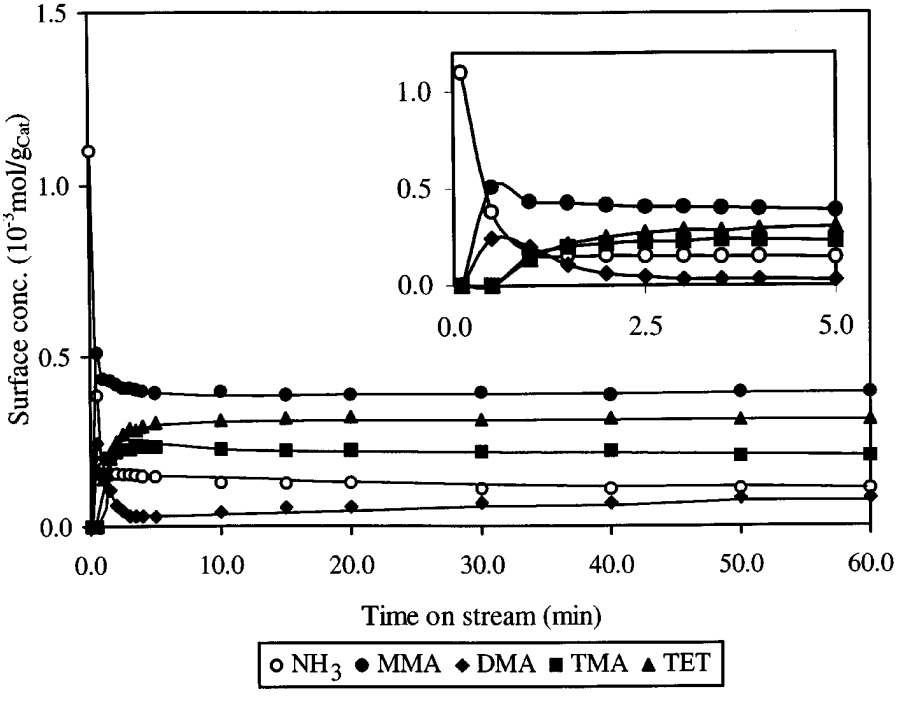

FIG. 5. Concentration of species sorbed on HMOR20-M under reactive conditions ($P_{(MeOH,NH_3)} = 5 \times 10^3$ Pa, $T = 633$ K) as a function of time on stream.

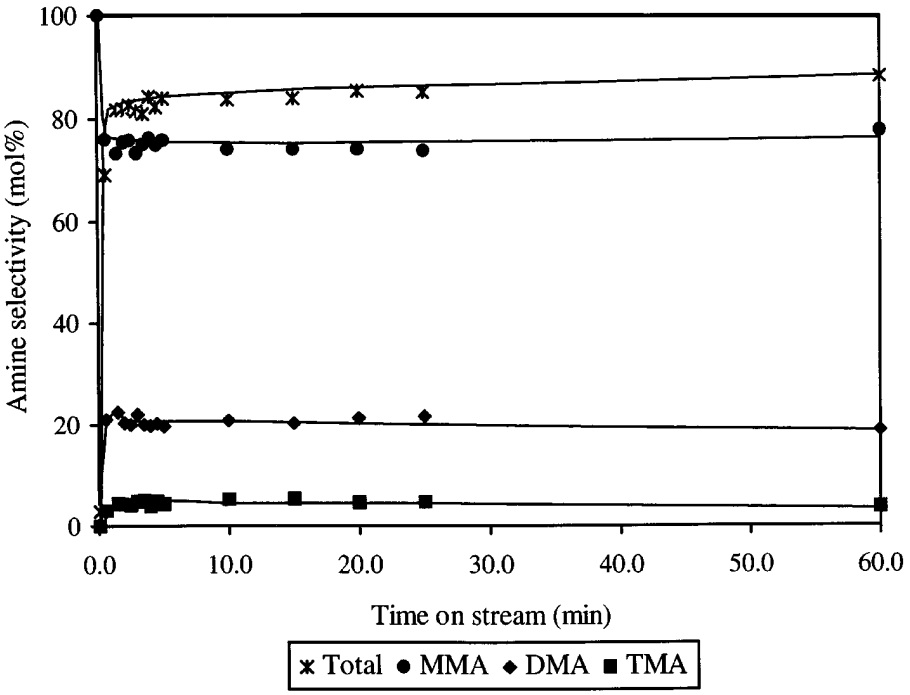

FIG. 6. Amine selectivity over HMOR20-M under reactive conditions ($P_{(MeOH,NH_3)} = 5 \times 10^3$ Pa, $T = 633$ K) as a function of time on stream.

Under these reaction conditions, the steady-state conversion based on methanol was 7%. At very short time on stream (<1 min), a high rate of methanol consumption was observed, and the main products were DME and hydrocarbons. With increasing time on stream, the formation of these by-products was quickly suppressed (Fig. 6), while the selectivity to methylamines increased (up to approximately 85% total amine selectivity at steady state). Then, the formation of DME was the only side reaction observed. It is interesting to note that presaturation of the catalyst with ammonia suppressed the high initial reactivity of the catalyst for the production of DME and hydrocarbons.

Among the methylamines, MMA was formed preferentially under these reaction conditions (75% selectivity). DMA and especially TMA were only found in very low concentrations, although a large fraction of the Brønsted acid sites of HMOR20-M (approximately 50%) was covered by the higher methylated ammonium ions (compare Fig. 5). Interestingly, deactivation of the formation of methylamines was not observed with increasing time on stream even though significant amounts of higher methylated amines were accumulated in the pores (and did not desorb).

Such a difference between the relative concentrations in the gas phase and in the zeolite pores was also observed for the parent HMOR20 (32). The relative steady-state concentrations of ammonia and the methylamines in the gas phase and on the surface of HMOR20 and HMOR20-M are depicted in Fig. 7. At low conversion, ammonia was present in large excess (>95% of all N-containing compounds) in the gas phase, and MMA was the favored reaction product over both catalysts. In the sorbed state, only ammonia and the lower substituted amines (i.e., MMA, DMA) were present in significant concentrations at steady state on HMOR20. In contrast, on HMOR20-M the concentration of TMA and TET exceeded that of the other sorbed species (NH_3, MMA, and DMA).

These results suggest that the higher methylated amines face diffusional constraints on the modified mordenite. Since under the chosen conditions reactive sorption of TMA was observed on the parent mordenite (32), only the rates of transport of MMA and DMA in both catalysts were studied. The fractional uptake of these amines on HMOR20 and HMOR20-M as a function of time is shown in Fig. 8. The rates of transport of MMA were comparable for both catalysts and the diffusion coefficients were calculated to be 4.5×10^{-13} and 5.5×10^{-13} cm^2/s in the parent and modified catalyst, respectively. In contrast, the rate of sorption of DMA was much smaller for HMOR20-M than for HMOR20, which is well reflected in the decrease of the diffusion coefficient by almost an order of magnitude (i.e., $d(\text{HMOR20}) = 3.0 \times 10^{-13}$ cm^2/s and $d(\text{HMOR20-M}) = 5 \times 10^{-14}$ cm^2/s).

DISCUSSION

Mechanistic Aspects of Methylamine Synthesis over Brønsted Acidic Mordenites

Prior to discussing the observed differences in selectivity for the synthesis of methylamines over HMOR20 and

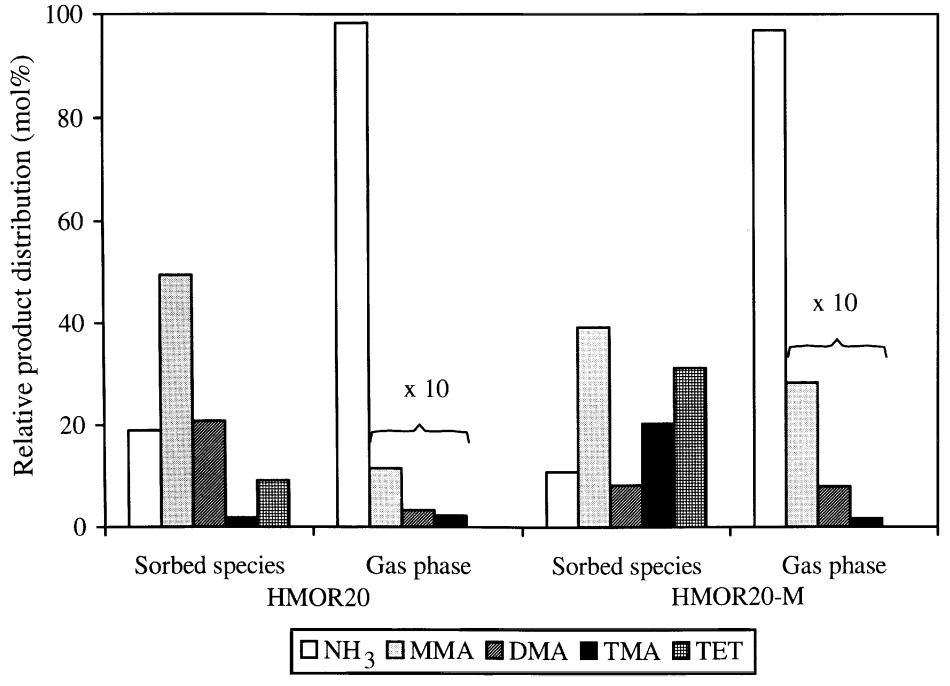

FIG. 7. Relative product distribution (obtained from the N mass balance) inside the pores of HMOR20 and HMOR20-M and in the gas phase ($P_{(MeOH,NH_3)} = 5 \times 10^3$ Pa, $T = 633$ K).

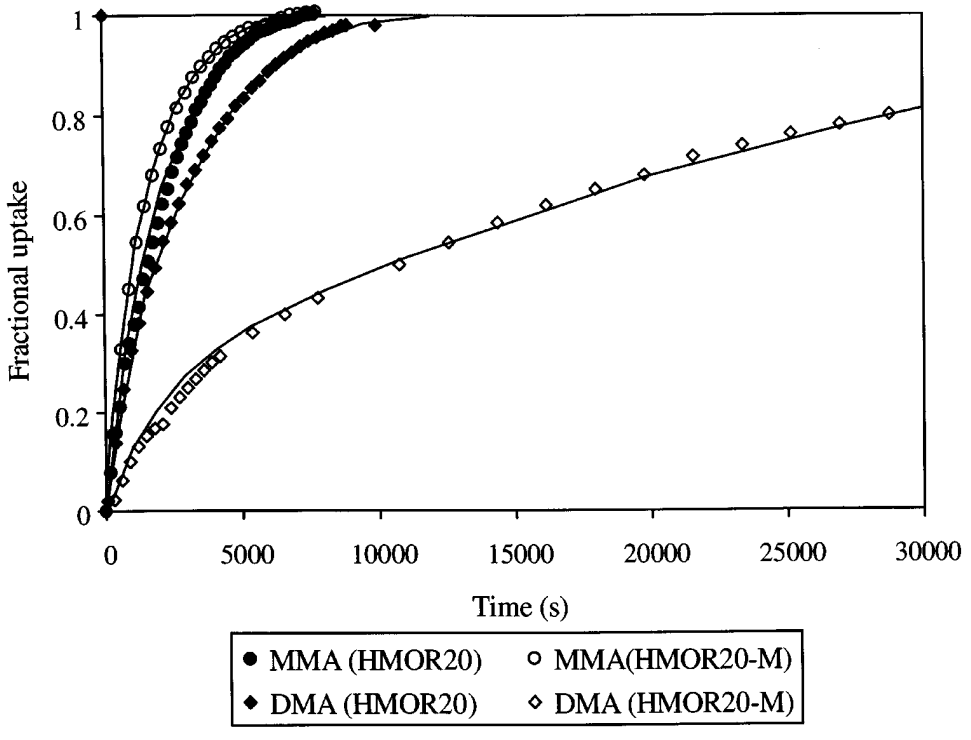

FIG. 8. Fractional uptake of MMA and DMA ($P = 10^{-1}$ Pa, $T = 308$ K) on HMOR20 and HMOR20-M as function of time.

HMOR20-M, it is important to describe the reaction pathways for the reaction of methanol with ammonia. These are similar for the two investigated catalysts and can be extended to a number of oxidic catalysts exhibiting high Brønsted acidity.

As reported earlier (32, 34), ammonia is preferentially adsorbed over methanol on Brønsted acidic zeolites under nonreactive conditions. Upon coadsorption, a complex is formed, in which methanol is weakly hydrogen bound to the free NH group of the sorbed ammonium ion. This complex is suggested to be the reactive precursor for the formation of chemisorbed methylamines, which involves a proton transfer from the ammonium ion (protonated amine) to the methanol, followed by a rapid release of water and the formation of the N–C bond via nucleophilic substitution. Due to the low attractive forces between the (methyl) ammonium ion and methanol in this coadsorption complex, only a low concentration is expected to be present at reaction temperature. This is consistent with the observations that under reaction conditions (i.e., at 633 K and 5×10^3 Pa of methanol and ammonia) sorbed methanol was not observed on Brønsted acidic mordenites (see Figs. 4 and 5).

At very short time on stream, the surface of H–mordenite is completely covered with ammonium ions, which are quickly displaced by chemisorbed methylamines. The methylammonium ions are formed in sequential order, up to the tetramethylammonium ion. Parallel experiments (in which the surface of Brønsted acidic mordenites was first saturated with ammonia and, then, only methanol was admitted) showed that the methylamines were also formed inside the zeolite pores, but that their rate of desorption was negligible when ammonia was not present in the feed stream (32). This is consistent with the findings of Chen *et al.* (35, 36), who calculated on basis of calorimetric studies that the rates of desorption of the amines at reaction temperature are several orders of magnitude lower than the observed rates of formation.

Thus, not the formation of the sorbed amines, but their release from their original adsorption sites into the gas phase is concluded to be involved in the rate determining step. This removal occurs via two different reaction pathways: (i) A chemisorbed amine is directly replaced from the surface by gas phase ammonia (methylamine) (*adsorption-assisted desorption mechanism*). (ii) A methylammonium ion in the pores reacts with gas phase ammonia (methylamine). This yields MMA (a higher substituted amine) in the gas phase and a lower substituted amine, (diminished by one methyl group) on the surface (*methyl-scavenging mechanism*). Whereas for chemisorbed MMA and DMA both pathways are feasible, the methyl scavenging mechanism seems to prevail for the removal of sorbed TMA and TET (32).

Assuming that the release of the amines from their sorption sites is rate determining, we would like to discuss the observed differences in the concentrations of sorbed methylammonium ions in the pores of the mordenites and the product distributions in the gas phase. The rapid formation of sorbed methylamines and their slow removal from the active sites allows all methylamines to be formed inside the pores. Their relative concentration strongly depends on the composition and morphology of the catalyst (37). Methylamines sorbed in the zeolites constitute then the reactive precursor for the formation of products, which are released into the gas phase. Thus, an increase in the partial pressure of ammonia, which facilitates the removal of the chemisorbed amines, can be expected to lead to an increase in activity. This is indeed found as the rate of methanol consumption on a particular catalyst increased, when the nitrogen to carbon ration of the reactant feed was raised. The increase in the ammonia to methanol ratio results in a large excess of gas phase ammonia in the zeolite pores (compared to the concentration of methylamines), which favors the formation of the lower substituted products, MMA and DMA (Fig. 3). Accordingly, a first order dependence of the methylamine formation on the ammonia partial pressure was found (36).

Enhanced Selectivity over HMOR20-M

The altered selectivity over the tetraethoxysilane modified mordenite (see Figs. 1 and 2) is illustrated by the reaction routes, along which the methylamine synthesis proceeds to thermodynamic equilibrium over the two catalysts (Fig. 9). For comparison, results for this reaction over amorphous silica–alumina catalysts, taken from Ref. (19), are included. Over HMOR20, thermodynamic equilibrium is approached similar to the route over the nonselective silica–alumina catalyst. Over HMOR20-M, however, the

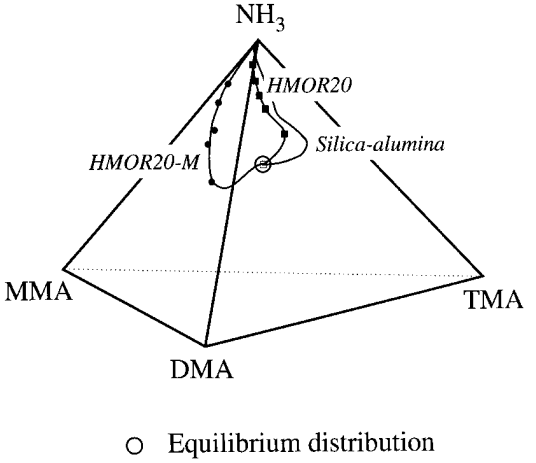

FIG. 9. Reaction routes for methylamine synthesis over HMOR20, HMOR20-M, and silica–alumina approaching thermodynamic equilibrium (N/C = 1, $T = 633$ K).

concentration of the lower substituted amines exceeds the corresponding equilibrium concentration at any conversion level. Note that due to the highly selective synthesis of MMA and DMA over this catalyst, an ammonia conversion exceeding the equilibrium value could be obtained under kinetically controlled conditions. Weigert observed a similar behavior for the methylamine synthesis over alkali exchanged mordenites, which catalyze MMA synthesis with high selectivity (19).

The following explanations for the observed enhancement in selectivity toward MMA and DMA over HMOR20-M are conceptually possible: (i) Modification with $Si(OEt)_4$ occurs throughout the mordenite crystals, leads to a narrowing of the pores, and, consequently, restricts the formation of the higher substituted amines (*restricted transition state selectivity*). Based on our results, this possibility can be ruled out because a high concentration of chemisorbed TMA and, even, TET was found in the pores under reaction conditions.

(ii) Modification with $Si(OEt)_4$ leads to a blocking of nonselective acid sites on the external surface of the zeolite crystals. This would lead to a decrease in activity for methylamine synthesis over the modified mordenite. Since the activity of the modified catalyst even increased slightly, we conclude that the number of acid sites on the external surface contributing to a nonselective amine formation is negligible.

(iii) Modification with $Si(OEt)_4$ occurs on the outer surface and results in only a narrowing of the pore openings, leading to a constraint for the diffusion of the higher methylated products in and out of the crystals (*diffusion controlled selectivity*). Indeed, a much lower diffusion coefficient for DMA was observed on HMOR20-M in comparison to HMOR20 under nonreactive conditions (Fig. 8). Segawa and Tachibana (27, 38) also observed a retardation in the rate of transport for DMA and complete suppression of sorption of TMA on mordenite treated with $SiCl_4$, whereas the diffusivities of NH_3 and MMA were essentially identical for both mordenites. This implies, that only the lower substituted amines (i.e., MMA and DMA) can diffuse out of the zeolite pore with a reasonable rate, although all methylamines are formed on the active sites. This, in turn, leads to an enrichment of the higher substituted amines inside the mordenite channels (i.e., TMA and TET) on HMOR20-M compared to the unmodified sample. These diffusional constraints, however, do not greatly affect the overall activity, because the rate of transport of MMA and DMA is still higher than their rate of formation.

Furthermore, significantly higher reaction rates for the methylation and transmethylation of MMA, DMA, and TMA compared to the methylation of ammonia were found (36). Based on the proposed reaction mechanism this can be attributed to the increasing base strength (facilitating the adsorption assisted desorption) and the higher nucleophilic character (facilitating the methyl scavenging mechanism) of higher substituted amines. Consequently, higher activity has to be expected, as their concentration inside the pores increases (i.e., on HMOR20-M due to the diffusional constraints).

Formation of Dimethyl Ether

At very short time on stream, the rate of DME formation was very high on Brønsted acidic mordenites and other by-products (i.e., hydrocarbons) were observed in the reaction of methanol and ammonia. This high initial activity is concluded to be associated with the transient period, during which ammonia is taken up by the mordenite catalyst. In this period, methanol reacts on free Brønsted acid sites via surface methoxy species (1). As the time on stream proceeded, all acid sites became covered with (methyl)ammonium ions, and, thus, the rate of DME formation decreased drastically. This is also consistent with the finding that this high initial rate of DME formation can be suppressed by pretreating the catalysts with ammonia prior to reaction.

At steady state, however, a fraction of methanol still is converted to DME. Its selectivity was found to depend on (i) the total methanol conversion, (ii) the N/C ratio of the feed, and (iii) the catalyst. Since surface-bound methoxy groups were not detected under reaction conditions, the formation of DME is speculated to proceed via a different reaction pathway. If one excludes that the formation of DME takes place on weaker acid sites (silanol groups) on the external surface (which can be excluded on basis of parallel experiments with silica containing a high concentration of silanol groups), the following reaction routes are plausible. (i) Protonated methanol, which is formed from methanol sorbed on (methyl)ammonium ions as proposed for the formation of surface bound methylamines, reacts with MeOH to form DME (17, 28). (ii) Chemisorbed amines react with MeOH to form DME similar to the formation of methylamines via the methyl-scavenging mechanism. Since both are competitive routes to the methylamine formation, a strong dependence of the selectivity toward DME on the relative concentration of NH_3 and MeOH is expected. Indeed, increasing the ammonia partial pressure relative to methanol (i.e., changing the N/C ratio of the feed) or decreasing the methanol concentration relative to ammonia (i.e., at high methanol conversion) resulted in a decrease in selectivity to DME.

However, one has to keep in mind that DME is also a reactive intermediate for the synthesis of methylamines over Brønsted acidic catalysts. Although the rate for the reaction of DME with ammonia is lower than for the reaction of MeOH with ammonia (36), this reaction route has to be considered when the concentration of DME and/or its residence time inside the pores increases.

CONCLUSIONS

Brønsted acidic mordenites are highly active for the synthesis of methylamines via the reaction of ammonia with methanol. Under reaction conditions, all Brønsted acid sites are covered with (methyl) ammonium ions. The formation of these chemisorbed amines occurs in sequential order, up to tetramethylammonium ions. The actual formation of these methylammonium ions, however, is not the rate-determining step in methylamine synthesis over Brønsted acidic zeolites. The overall reaction rate is determined by their release from the adsorption sites into the gas phase. This occurs via two reaction pathways, i.e., ammonia (methylamines) adsorption-assisted desorption and/or scavenging of methyl groups of chemisorbed amines by ammonia (methylamines).

The product distribution strongly depends on the total methanol conversion and on the ammonia to methanol ratio of the feed. Furthermore, it is significantly altered by modification of the Brønsted acidic mordenite with tetraethoxysilane. Whereas over the unmodified catalyst, the equilibrium distribution of the methylamines is approached via a similar pathway as found over nonselective, amorphous catalysts, the selectivity toward the lower substituted amines (i.e., MMA and DMA) is greatly enhanced over the modified mordenite. Because the higher alkylated methylamines (i.e., TMA and TET) are present in high concentrations within the zeolite pores, restrictions in the transition state to form these amines cannot be responsible for their lower gas phase concentrations. Thus, we conclude that the modification imposes constraints for the diffusion of these higher methylated amines by narrowing the pore entrances. The causes significantly prolonged residence times for the bulkier products. They, then, undergo rapid methyl scavenging resulting in a high selectivity to mono- and dimethylamine.

ACKNOWLEDGMENTS

We are grateful to the Christian Doppler Society for partial support of the work and to the Japanese Catalysis Society for providing the mordenite samples.

REFERENCES

1. Chang, C. D., "Hydrocarbons from Methanol." Dekker, New York, 1983.
2. Hölderich, W. F., and van Bekkum, H., *Stud. Surf. Sci. Catal.* **58**, 631 (1991).
3. Hölderich, W. F., *in* "Guidlines for Mastering the Properties of Molecular Sieves" (D. Barthomeuf *et al.*, Eds.), p. 319. Plenum, New York, 1990.
4. Weisz, P. B., *Pure Appl. Chem.* **52**, 2091 (1980).
5. Derouane, E. G., *Stud. Surf. Sci. Catal.* **5**, 5 (1980).
6. Dwyer, J., and Dyer, A., *Chem. Ind.* **265**, 237 (1984).
7. Haag, W. O., *in* "Heterogeneous Catalysis" (B. L. Shapiro, Ed.), Vol. 2, p. 95. Texas A&M Univ. Press, College Station, TX, 1984.
8. Chen, N. Y., Degnan, T. F., Jr., and Smith, C. M., "Molecular Transport and Reactions in Zeolites." VCH, New York, 1994.
9. Weisz, P. B., Frilette, V. J., Maatman, R. W., and Mower, E. B., *J. Catal.* **1**, 307 (1962).
10. Mirth, G., and Lercher, J. A., *J. Catal.* **132**, 244 (1991).
11. Mirth, G., Cejka, J., and Lercher, J. A., *J. Catal.* **139**, 24 (1993).
12. Csicsery, S. M., *J. Catal.* **23**, 124 (1971).
13. Turcotte, M. G., and Johnson, T. A., *in* "Kirk-Othmer Encyclopedia of Chemical Technology" (J. I. Kroschwitz, Ed.), 4th ed., Vol. 2, p. 369. Wiley, New York, 1992.
14. van Gysel, A. B., and Musin, W., *in* "Ullmann's Encyclopedia of Industrial Chemistry" (B. Elvers, S. Hawkins, and G. Schultz, Eds.), 5th ed., Vol. A16, p. 535. VCH, Weinheim, 1990.
15. Pesce, L. D., and Jenks, W. R., *in* "Riegel's Hanbook of Industrial Chemistry" (J. A. Kent, Ed.), 9th ed., p. 1109. Van Nostrand–Reinold, New York, 1992.
16. Deeba, M., and Cochran, R. N., European Patent Application 85.408, 1983.
17. Mochida, I., Yasutake, A., Fujitsu, H., and Takeshita, K., *J. Catal.* **82**, 313 (1983).
18. Ashina, Y., Fujita, T., Fukatsu, M., Niwa, K., and Yagi, J., *Stud. Surf. Sci. Catal.* **28**, 779 (1986).
19. Weigert, F., *J. Catal.* **103**, 20 (1987).
20. Abrams, L., Corbin, D. R., and Shannon, R. D., European Patent Application 251.597, 1987.
21. Shannon, R. D., Keane, M., Jr., Abrams, L., Staley, R. H., Gier, T. E., Corbin, D. R., and Sonnichsen, G. C., *J. Catal.* **113**, 367 (1988).
22. Shannon, R. D., Keane, M., Jr., Abrams, L., Staley, R. H., Gier, T. E., and Sonnichsen, G. C., *J. Catal.* **115**, 79 (1989).
23. Shannon, R. D., Keane, M., Jr., Abrams, L., Staley, R. H., Gier, T. E., Corbin, D. R., and Sonnichsen, G. C., *J. Catal.* **114**, 8 (1988).
24. Niwa, M., Kato, S., Hattori, T., and Murakami, Y., *J. Chem. Soc. Faraday Trans. 1* **80**, 3135 (1984).
25. Bergna, H. E., Keane, M., Jr., Ralston, D. H., Sonnichsen, G. C., Abrams, L., and Shannon, R. D., *J. Catal.* **115**, 148 (1989).
26. Corbin, D. R., Keane, M., Jr., Abrams, L., Farlee, R. D., Biersted, P. E., and Bein, T. E., *J. Catal.* **124**, 268 (1990).
27. Segawa, K., and Tachibana, H., *J. Catal.* **131**, 482 (1991).
28. Fetting, F., and Dingerdissen, U., *Chem. Eng. Technol.* **15**, 202 (1992).
29. Kiyoura, T., and Terada, K., European Patent Application 593.086, 1994.
30. Sawa, M., Niwa, M., and Murakami, Y., *Zeolites* **10**, 532 (1990).
31. Mirth, G., Eder, F., and Lercher, J. A., *Appl. Spectrosc.* **48**, 194 (1994).
32. Gründling, Ch., Eder-Mirth, G., and Lercher, J. A., *Res. Chem. Intermed.,* in press.
33. Crank, J., "The Mathematics of Diffusion," 2nd ed. Clarendon, Oxford, 1975.
34. Kogelbauer, A., and Lercher, J. A., *J. Chem. Soc. Faraday Trans.* **88**, 2283 (1992).
35. Chen, D. T., Zhang, L., Chen, Y., and Dumesic, J. A., *J. Catal.* **146**, 257 (1994).
36. Chen, D. T., Zhang, L., Kobe, J. M., Chen, Y., and Dumesic, J. A., *J. Mol. Catal.* **93**, 337 (1994).
37. Gründling, Ch., Eder-Mirth, G., and Lercher, J. A., manuscript in preparation.
38. Segawa, K., and Tachibana, H., *in* "Proceedings of the 10th ICC" (Guczi *et al.*, Eds.), p. 1273. Elsevier, Amsterdam, 1993.